

Estimation of Surface Dose in the Presence of Unwanted Air Gaps under the Bolus in Postmastectomy Radiation Therapy: A Phantom Dosimetric Study

Lobo Dilson, Srinivas Challapalli*, Banerjee Sourjya, MS Athiyamaan, Ravichandran Ramamoorthy, Sunny Johan, Krishna Abhishek

Abstract

Background: The aim of this study is to design and fabricate a thorax phantom with irregularly shaped trapezoidal slots across the left side of the chest wall, allowing for the creation of unwanted air gaps under the bolus. **Method:** Surface dose (D_{surf}) measurements were made with Gaf Chromic EBT3 films at air gaps (0.0, 5.0, 10.0 and 15.0 mm) under gel bolus of thickness (5.0 mm & 10.0 mm), for 3DCRT technique (2 and 3 field) with clinical 6 MV photon beam under uniform and non-uniform air gap condition. The obtained values were compared with TPS estimated ones. **Results:** In the presence of 15.0 mm uniform air gap, the mean estimated and measured D_{surf} values with two and three field techniques decreased by 14.0 % to 15.2% and 14.7% to 17.4% under 5.0 mm and 10.0 mm bolus applications respectively. In presence of non-uniform air gap condition, the effect on D_{surf} was minimal (3 to 3.5%) compared with the uniform air gap condition. **Conclusions:** Based on the study's findings, it is recommended that when using bolus in clinical radiotherapy applications, special care be taken to avoid unwanted air gaps under the bolus in order to achieve a uniform surface dose across the treatment region, where a customized 3D printed bolus may be a better option.

Keywords: Air gap- bolus- PMRT- Thorax Phantom

Asian Pac J Cancer Prev, 23 (9), 2973-2981

Introduction

Megavoltage (MV) photon beams, which have a dose-build-up effect, are commonly used in clinical radiotherapy treatments (Buston et al., 2000). The lack of electron equilibrium results in reduction of surface dose (D_{Surf}), which is known as "the skin sparing effect" with these beams (Bilge et al., 2009). The D_{Surf} depend on beam properties such as energy spectrum, field size, source to surface distance, angle of incidence and treatment head design that produces the secondary electrons etc. (Boman et al., 2000). With 6 MV photon beam, it is estimated that D_{Surf} can be as low as 25% of the depth of maximum dose (d_{max}) developed at a depth (Khan et al., 2013). Though the ability to spare the skin is extremely advantageous for a wide range of clinical radiotherapy treatments, the D_{Surf} could be a critical parameter to the outcome when treating superficial targets near the skin's surface, such as post-mastectomy radiotherapy (PMRT) or head and neck cancer treatments. In these treatments, a layer of tissue equivalent material known as a "bolus" is placed directly on the patient's treatment surface, benefiting to increase D_{Surf} and the dose uniformity (Buston et al., 2000).

Because of the malleability of the bolus material and the treatment surface irregularity, accurate fitting to the surface may not be feasible that causes an unwanted air gaps between the bolus and skin surface, results in decrease of D_{Surf} (Sakai et al., 2021; Robar et al., 2018; Jreije et al., 2021). Accurate measurement of D_{Surf} in radiotherapy can provide a valuable information for clinical use to avoid near surface recurrences while at the same time limiting severe skin toxicity (Boman et al., 2018; Ha et al., 2016).

Several studies (based on phantom or patient) have reported on the impact of D_{Surf} with different thickness of air gaps under the bolus in several treatment techniques. Sakai Y et al. (Sakai et al, 2021) found that the mean maximum air gap thickness with 5.0 mm gel bolus application from seven PMRT patients was $9.9 \text{ mm} \pm 2.8 \text{ mm}$. According to Robar JL et al. (Robar et al, 2018), approximately 30% of all treatment fractions had an air gap of greater than 5.0 mm, with maximum of 17.0 mm (approx.) was measured by cone beam computed tomography (CBCT) from 16 PMRT patients' data with 5.0 mm gel bolus application. They have shown that the larger air gaps occurred at regions of irregular surface

locations featuring more convexities or concavities. From the study done with thorax phantom on customized 3D printed bolus for breast reconstruction for radical mastectomy, Ha Jin-Suk et al. (Ha et al, 2016) reported that the minimum and maximum values of the air gap using commercialized-bolus were 8.0 mm and 15.0 mm respectively.

The effect of D_{surf} in presence of uniform air gap under the bolus was addressed in several studies (Buston et al., 2000; Boman et al., 2000; Khan et al., 2013; Madhavi et al., 2015; Chung et al., 2013). Though this situation is unlikely will occur in routine clinical situations, there is a need to analyze the effect of D_{surf} at clinically relevant air gaps under gel bolus application in PMRT.

In this study, an attempt was made to design and fabricate a thorax phantom with irregularly shaped slots across the left side of the chest wall, allowing for the creation of unwanted air gaps under the bolus. The effect of air gap under the bolus on surface dose was investigated with uniform and non-uniform air gap condition in phantom.

Materials and Methods

Treatment unit and film calibration

All irradiations were carried out using a medical linear accelerator (M/s Elekta AB, Stockholm, Sweden, Model: Compact) with a photon mode of 6 MV and a beam quality index of 0.667. This unit has motorized physical wedge (600), 40 pairs multi-leaf collimator (MLCi2) with leaf thickness of 1.0 cm at 100 cm iso-center, operating with a dose rate of 350 MU/min. The beam output is calibrated to 1cGy/MU at iso-center as per TRS-398 protocol (IAEA, 2000). All the measurements in this study were carried out with GafChromic EBT3 film (International Specialty Products, Wayne, New Jersey, USA; Lot No. 09071703) which has been proven to be a viable tool for MV radiation dosimetry (Casanova et al, 2013; Chiu-Tsao et al, 2012). The product was suitable to surface measurement near build-up region due to thin configuration (thickness of ~ 0.278 mm) and near-tissue equivalence (Chiu-Tsao et al, 2012). The process of calibration of EBT3 film, its scan protocol and to obtain dose readings from irradiated film, were followed as stated by Lobo et al (Lobo et al, 2019).

Design and fabrication of thorax phantom

The design and fabrication of thorax phantom is as mentioned by Lobo D et al. (Lobo et al., 2021). This phantom was fabricated locally to confirm the delivered dose to the target (chest wall) as well as the surface dose to the scar region with 3DCRT plans for PMRT patients. Thirty acrylic plates (density $\approx 1.04 \text{ g/cm}^3$) were cut into elliptical shape with 21.0 cm height and 31.0 cm in width, of thickness 1.0 cm each. Provisions were made to insert lung equivalent cork material (density $\approx 0.28 \text{ g/cm}^3$) towards the left and right side. A few slots were created in the phantom, one to insert bone equivalent Teflon material (density $\approx 1.65 \text{ g/cm}^3$) to simulate the spine, within which provision to insert a miniature ionization chamber (Model CC13, M/s IBA Dosimetry, Germany) and another slot at the representative

position of the esophagus to insert a farmer type ionization chamber (Model FC65, M/s IBA Dosimetry, Germany). Three chamber slots (CH1: medial; CH2: medio-lateral & CH3: lateral) to insert CC13 ionization chambers towards the right chest wall target region were also made. Chamber slots in chest wall region are covered with acrylic rods unless measurements were made. Figure 1a shows the schematic diagram of frontal view with dimensions of the thorax phantom having lung (right and left), spine, and chamber slots, as well the position of the three nylon nuts.

Taking into consideration the concavities at various locations on the irregular surface of PMRT patients who were treated with bolus as reported in the literature, a trapezoidal-shaped slot with dimensions of 2.0 cm (lower base), 1.5 cm (height), and 3.0 cm (larger base) cm was created on nine acrylic plates across the left side of the chest wall at medial (A) location in three plates, medio-lateral (B) location in three plates, and lateral (C) location in three plates. This slot is meant to simulate the air gap under bolus and to place EBT3 film (2.0 cm \times 2.0 cm) at the base of slot for surface dose estimation. The maximum height of air gap of 1.5 cm was chosen based on the maximum thickness of air gap under gel bolus observed, as reported in the literature. Figure 1b shows schematic representation of frontal view of thorax phantom with three (A, B and C) trapezoidal slot locations across the left side of chest wall.

All thirty acrylic plates with lung, spine, and acrylic rods in the chamber slots were stacked together on the front and back of the phantom using three threaded acrylic rods of 2.0 cm diameter and nylon nuts, so that the superior part consists of fifteen plates having uniform curved surface towards left side of chest wall, followed by the inferior part consisting of fifteen plates having combination of plates with trapezoidal-shaped slot across the left side chest wall. Perspective view of frontal, right and left side of the fabricated thorax phantom is shown in Figure 2a, 2b & 2c respectively. Placement of EBT3 film locations at superior and inferior part is seen in Figure 2c.

Computed Tomography (CT) simulation

The phantom was scanned using a computerized tomography (CT) (M/s Wipro GE 'High Speed') unit with 2.5 mm slice thickness and an image matrix of 512 \times 512. Several transverse imaging CT sets were obtained for the phantom's superior and inferior parts keeping the scanning parameters consistent across all sets. For surface dose estimations and measurements, film locations were marked towards left side of chest wall at superior and inferior parts of the phantom. Fiducial markers were placed along the marked film locations in the middle portion of the superior part of the phantom and at trapezoidal base slots (A, B and C) located at inferior part of the phantom for identification of film location in the treatment planning system (TPS) and for surface dose estimations and measurements. Water equivalent Superflab gel bolus of thicknesses of 5.0 mm and 10.0 mm were used during CT simulation process over superior and inferior part of the phantom and execution of treatment plans in this study.

CT simulation - Superior part of the phantom

Nine CT imaging data sets were obtained for superior part of the phantom. One set corresponding with nil bolus and the remaining sets by placing an air equivalent sheet (foam roll) of thickness 0.0 mm, 5.0 mm, 10.0 mm, and 15.0 mm with 5.0 mm and 10.0 mm bolus placement respectively (simulating the uniform air gap thickness under bolus) were taken. The purpose to take these imaging sets is to study the effect of D_{surf} with uniform air gap under 5.0 mm and 10.0 mm gel bolus applications. Figure 3a represents the superior portion of the phantom simulating a uniform air gap under gel bolus towards left side chest wall. Table 1 represents CT imaging data set numbers using various thicknesses of gel bolus and an air equivalent sheet taken with superior part (uniform surface geometry towards left side) of the thorax phantom.

CT simulation - Inferior part of the phantom

Three CT imaging data sets were obtained for inferior part of the phantom. One without placement of bolus, and the remaining ones by placing the 5.0- and 10.0-mm gel bolus on top of the phantom surface. Figure 3b represents the schematic diagram representing the inferior part of phantom having trapezoidal shaped cuts as air gaps at three different locations under gel bolus. Table 2 represents the description of CT imaging data set numbers using various thicknesses of gel bolus and an air equivalent sheet taken with inferior part (non-uniform surface geometry towards left side having trapezoidal slots) of the thorax phantom.

Figure 3a shows transverse CT image data sets of the superior part of the thorax phantom done as per Table 1 with uniform surface towards the left side of the chest wall under nobolus, 5.0 mm and 10.0 mm actual bolus applications, and 0.0 mm, 5.0 mm, 10.0 mm, and 15.0 mm uniform air gap under the bolus to the surface.

Figure 3b shows transverse CT image data sets of the inferior part of the thorax phantom with non-uniform surface (having trapezoidal slots at locations A, B, and C) towards the left side of the chest wall with nobolus, 5.0 mm and 10.0 mm virtual and actual bolus applications, respectively. Under actual bolus (of thickness 5.0 mm and 10.0 mm) applications, an air gap of thickness 15.0 mm been seen at all three (A, B and C) slot locations.

Target and OAR delineation

All image data sets were exported to a Focalsim contouring station (M/s Elekta Ltd., Crawly, Germany). Surface contour of phantom, planning target volume (PTV) towards the left side of phantom and the organ at risk (lung) was drawn by the radiation oncologist. PTV was cropped by 1.0 mm below the surface contour of phantom (shown in Figure 1a and 1b). Contouring of PTV as appropriate was performed using the RTOG guidelines for the radio-therapeutic treatment of PMRT patients (Cox et al., 1995). Following the treatment planning protocol for PMRT treatments at our institute, a skin flash was generated with a margin of 10.0 mm towards the anterior and left lateral sides of PTV to account for breathing movements.

3DCRT planning and D_{surf} estimates

Contoured CT image data sets of thorax phantom were transferred to TPS (model CMS XiO®, Elekta Ltd, Crawly, UK, version 4.80.02) for dose calculations using superposition algorithm. Taking each CT data set, two 3DCRT plans were generated by taking the center of the target as the iso-centre. First one by using tangential pair beams having field dimensions of 6 cm × 12 cm (two field technique), and the second one having two tangential beams with field dimensions 6 cm × 12 cm followed by one left anterior oblique beam (three-field technique). Tangential beams were conformed to the skin flash with a 0.5 cm margin. A dose prescription of 50 Gy in 25 fractions was normalized to the 100% iso-dose line in all plans, giving equal weight to all the beams. The weight point was placed at an appropriate location inside the PTV to achieve a 95% of prescription dose across the target. To avoid the uncertainties associated among the plans, field in field technique was avoided.

To figure the dose difference between estimated by TPS and EBT3 measurement, point dose at skin surface on CT image was used to represent the surface dose calculated by TPS. In each plan, ten interest points below 1.0 mm of skin contour were placed across the marked location of the film in TPS for estimation of D_{surf} . Their respective coordinates were kept consistent across all 3DCRT plans generated from all CT sets. If bolus material or virtual bolus was used, the point dose would be obtained from the interface between bolus and skin contour.

Virtual bolus of thicknesses 5.0 mm and 10.0 mm was used in TPS while generating 3DCRT plans with CT set no.10 for calculation of D_{surf} simulating no-air gap condition under bolus. The mean dose at these interest points calculated by TPS was noted as $D_{surf, tps}$. A layer of Gafchromic EBT3 film was taped to the surface of the irradiated area of thorax phantom to estimate/measure the surface dose received. All 3DCRT plans were executed under linear accelerator, placing the actual bolus (as done in CT simulation) and EBT3 films at appropriate locations. The measured mean surface dose with films was noted as $D_{surf, film}$. Each 3DCRT plan was executed three times under linac, and the mean surface dose values obtained were recorded. The $D_{surf, tps}$ and $D_{surf, film}$ values were expressed as percentage of prescription dose unless otherwise specified.

Air gaps (AG) of thickness 0.0 mm, 5.0 mm, 10.0 mm, and 15.0 mm under 5.0 mm and 10.0 mm boluses were abbreviated as AG0 (5), AG5 (5), AG10 (5), and AG15 (5); AG0 (10), AG5 (10), AG10 (10), and AG15 (10), respectively, and surface was tabulated against each air gap for analysis towards superior part of phantom. Similarly, air gaps thickness 0.0 mm, and 15.0 mm under 5.0 mm and 10.0 mm boluses at A, B and C slots towards inferior part of the phantom were abbreviated as No Bolus (A), No Bolus (B), No Bolus (C); AG0A (5), AG0B (5), AG0C (5); AGA15(5), AGB15 (5), AGC15 (5); AG0A (10), AG0B (10), AG0C (10); AGA15 (10), AGB15 (10), AGC15 (10) respectively.

Results

Surface dose under bolus

Table 3 shows the surface dose (Mean±SD) values ($D_{surf, tps}$ & $D_{surf, film}$) under nil (0.0 mm), 5.0 mm and 10.0 mm thickness of gel bolus in two and three field treatment techniques at superior and inferior (A, B and C slots) portion of thorax phantom.

With superior portion of phantom, in two field treatment technique, under nil (0.0 mm), 5.0 mm and 10.0 mm gel bolus applications, the mean $D_{surf, tps}$ and $D_{surf, film}$ were 60.8%, 93.3% and 103.2%; 58.1%, 88.4% and 94.1% respectively. Similarly, with three field technique the mean $D_{surf, tps}$ and $D_{surf, film}$ were 61.3%, 90.3% and 103.3%; 61.2%, 88.7% and 96.1% respectively under nil, 5.0 mm, and 10.0 mm bolus application.

With inferior portion of phantom, in two field treatment technique, under 0.0 mm, 5.0 mm and 10.0 mm gel bolus applications, the $D_{surf, tps}$ values were 63.4%, 93.5% and 98.7%; 64.5%, 95.8% and 100.3%; 63.4%, 93.5% and 98.7% at slots A, B and C respectively. Similarly, with three field technique $D_{surf, tps}$ values were 67.1%, 95.2% and 100.5%; 68.2%, 97.6% and 102.8% ; 67.1%, 95.2% and 100.5% at slots A, B and C respectively. However the obtained $D_{surf, film}$ values for two and three field techniques

under no bolus conditions were 58.1%, 59.3% and 58.6%; 67.6%, 66.4% and 65.8% respectively at slots A, B and C. Measurements could not be done for 5.0 mm and 10.0 mm bolus in contact condition due to non-availability of 3D printed bolus.

Surface dose under uniform air gap condition

Figure 4 (a to d) represents the whisker plots of $D_{surf, tps}$ and $D_{surf, film}$ surface doses measured in presence of uniform air gap condition under No bolus, 5.0 mm and 10.0 mm bolus application with two and three field technique. There is reduction in surface dose as air gap thickness increases from 0.0 mm to 15.0 mm under both bolus thicknesses and treatment techniques as observed from these figures.

Table 4 represents, the reduction in surface dose under 5.0 mm and 10.0 mm bolus thicknesses without and with uniform air gap in two field and three field treatment techniques towards superior portion of thorax phantom. As the air gap between the bolus and surface increased from 5.0 mm to 15.0 mm, the $D_{surf, tps}$ value decreased from 4.7 to 14.0% & 6.1 to 15.2% for 2 field technique and 4.9 to 14.7% & 6.9 to 17.4% for 3 field technique under 5.0 mm and 10.0 mm bolus applications respectively. Similarly, the decrement in $D_{surf, film}$ followed the same trend as shown in Table 4.

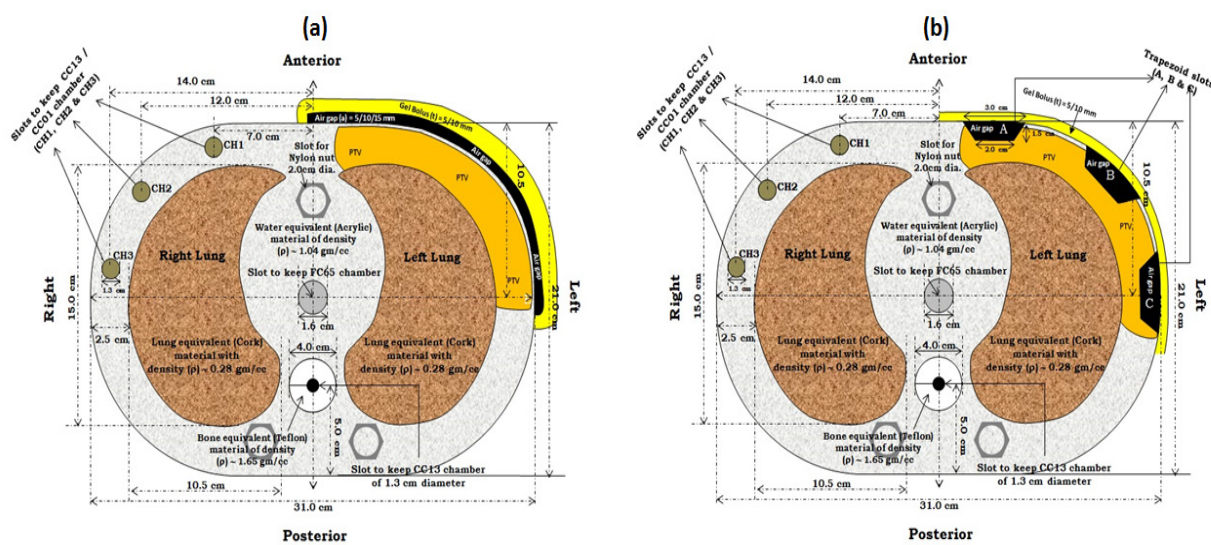


Figure 1. Schematic Diagram of Frontal View of Thorax Phantom Having (a) Uniform Surface and (b) Non Uniform Surface Towards Left Side with Bolus and Target (PTV). The air gap under bolus in both diagrams is seen.

Table 1. CT Imaging Data Set Numbers Using Various Thicknesses of Gel Bolus and an Air Equivalent Sheet Taken with Superior Part (uniform surface geometry towards left side of the chest wall) of the Thorax Phantom

Surface geometry	CT imaging data set number	Air equivalent sheet thickness (in mm)	Gel bolus thickness (in mm)
Uniform (left side)	1	0	0
	2	0	5
	3	0	10
	4	5	5
	5	5	10
	6	10	5
	7	10	10
	8	15	5
	9	15	10

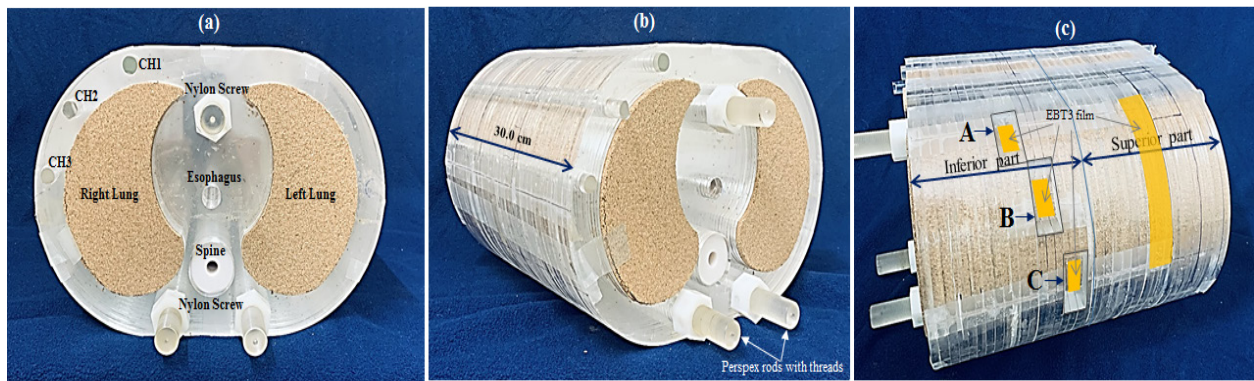


Figure 2. Perspective View of (a) Frontal, (b) Right and (c) Left Side of the Fabricated Thorax Phantom

Table 2. CT Imaging Data Set Numbers Using Various Thicknesses of Gel Bolus Taken with Inferior Part (non-uniform surface geometry towards left side of chest wall having trapezoidal slots) of the Thorax Phantom.

Surface geometry	CT imaging data set number	Trapezoidal slots height at three different locations A, B & C (in mm)	Gel bolus thickness (in mm)
Non-uniform (left side)	10	0	0
	11	15	5
	12	15	10

Surface dose under non-uniform air gap condition

Figure 5 (a to d) represents the whisker plots of $D_{surf, tps}$ and $D_{surf, film}$ surface doses measured in presence of non-uniform air gap condition under No bolus, 5.0 mm and 10.0 mm bolus application with two and three field technique at slots A, B and C. As observed from the figure, there is reduction in surface dose as air gap thickness increases from 0.0 mm to 15.0 mm under both bolus and treatment techniques. As the measurement could not be obtained with bolus in contact condition (simulating virtual bolus) measured surface dose comparison could not be analyzed shown in Figure 5b and 5d.

Table 5 represents the reduction of surface dose ($D_{surf, tps}$ and $D_{surf, film}$) under 5.0 mm and 10.0 mm bolus thicknesses without and with air gap observed in two field and three field treatment techniques towards inferior portion of thorax phantom at three slots A, B and C. As observed from the table, with the increase of air gap from

0.0 mm to 15.0 mm, the $D_{surf, tps}$ decreased by 3.5% and 3.0% at air gaps under all three slots for 5.0 mm and 10.0 mm bolus applications in two and three field techniques respectively.

Discussion

The D_{surf} in the presence of air gaps (uniform and non-uniform) under different thicknesses of gel bolus in a locally fabricated thorax phantom using 3DCRT techniques was investigated in this study.

Though the calculation of D_{surf} by TPS is inaccurate, the precise measurement of D_{surf} can offer significant information in preventing recurrences near the surface and limiting serious skin toxicity (Sakai et al., 2021; Robar et al., 2018). Gina Wong et al. (Wong et al., 2020) found that the TPS calculated mean surface dose without and with 5.0 mm bolus application was 65% and 95% from

Table 3. Surface Dose (Mean±SD) values ($D_{surf, tps}$ & $D_{surf, film}$) Under Nil (0.0 mm), 5.0 mm and 10.0 mm Thickness of Gel Bolus in Two and Three Field Treatment Techniques at Superior and Inferior (A, B and C slots) Portion of Thorax Phantom

Bolus thickness (in mm)	Treatment technique	Surface dose (%)							
		Superior portion				Inferior portion			
		A		B		C			
		$D_{surf, tps}$	$D_{surf, film}$	$D_{surf, tps}$	$D_{surf, film}$	$D_{surf, tps}$	$D_{surf, film}$	$D_{surf, tps}$	$D_{surf, film}$
0	2 field	60.8 ± 4.8	58.1 ± 4.5	63.4 ± 2.6	58.1 ± 4.5	64.5 ± 3.1	59.3 ± 2.3	63.4 ± 2.6	58.6 ± 1.8
	3 field	61.3 ± 6.2	61.2 ± 2.7	67.1 ± 2.3	67.6 ± 4.7	68.2 ± 3.2	66.4 ± 4.4	67.1 ± 2.3	65.8 ± 3.3
5	2 field	93.3 ± 3.3	88.4 ± 3.4	#93.5 ± 2.0	*	#95.8 ± 2.0	*	#93.5 ± 2.0	*
	3 field	90.3 ± 1.7	88.7 ± 4.8	#95.2 ± 1.7	*	#97.6 ± 1.7	*	#95.2 ± 1.7	*
10	2 field	103.2 ± 1.9	94.1 ± 4.2	#98.7 ± 1.5	*	#100.3 ± 2.5	*	#98.7 ± 1.3	*
	3 field	103.3 ± 2.0	96.1 ± 2.3	#100.5 ± 1.2	*	#102.8 ± 1.2	*	#100.5 ± 1.2	*

SD, Standard deviation; # Values obtained with virtual bolus application from TPS (Refer CT Set No.10); * Measurement was not made as virtual bolus condition could not be simulated due to non-availability of 3D printed bolus.

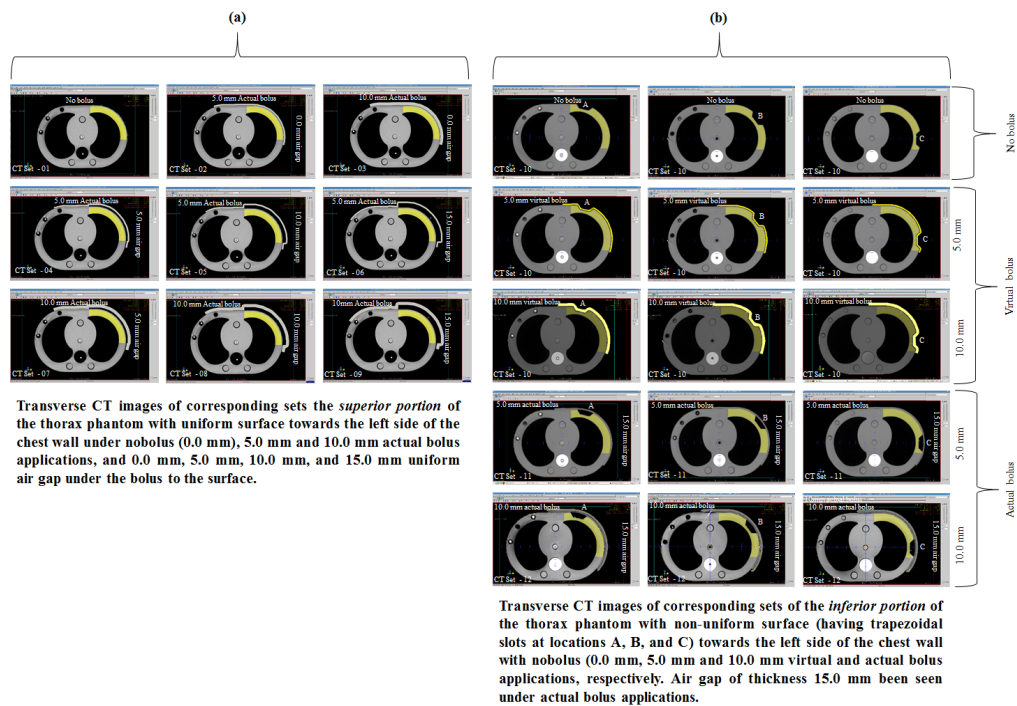


Figure 3. Transverse CT Image Sets the (a) Superior and (b) Inferior Portion of Thorax Phantom Having Air Gap under Bolus

a group of 44 PMRT patients scheduled for tangential irradiation technique. Fiedler DA et al. (Fiedler et al., 2021) reported that from the planned tangential field in field 3DCRT techniques, the TPS calculated and EBT3 measured surface dose obtained from a chest phantom without, with 5.0 mm, 10.0 mm bolus applications were

60.6±11.7% and 63.7±3.0%; 97.2±1.1% and 96.8±2.8%; 96.4±1.7% and 94.4±3.5% respectively [17] Ordonez-Sanz C et al. (Ordonez-Sanz et al., 2014) reported the TPS calculated and TLD measured surface dose under tangential irradiation technique without bolus application was 76.5% and 68.0% respectively. Our

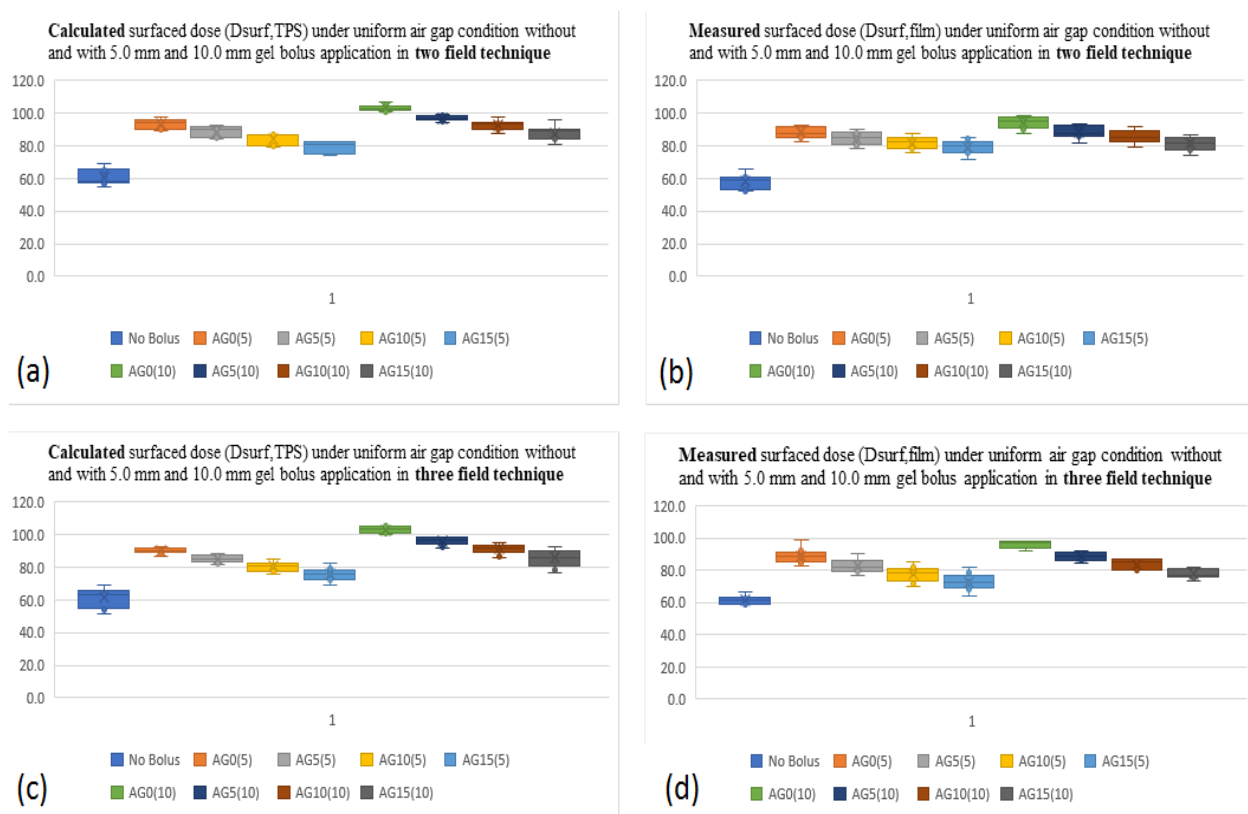


Figure 4. (a to d) Represents the Whisker Plots of $D_{surf,TPS}$ and $D_{surf,film}$ Surface Doses Measured in Presence of Uniform Air Gap Condition under No Bolus, 5.0 mm and 10.0 mm Bolus Application with Two and Three Field Technique

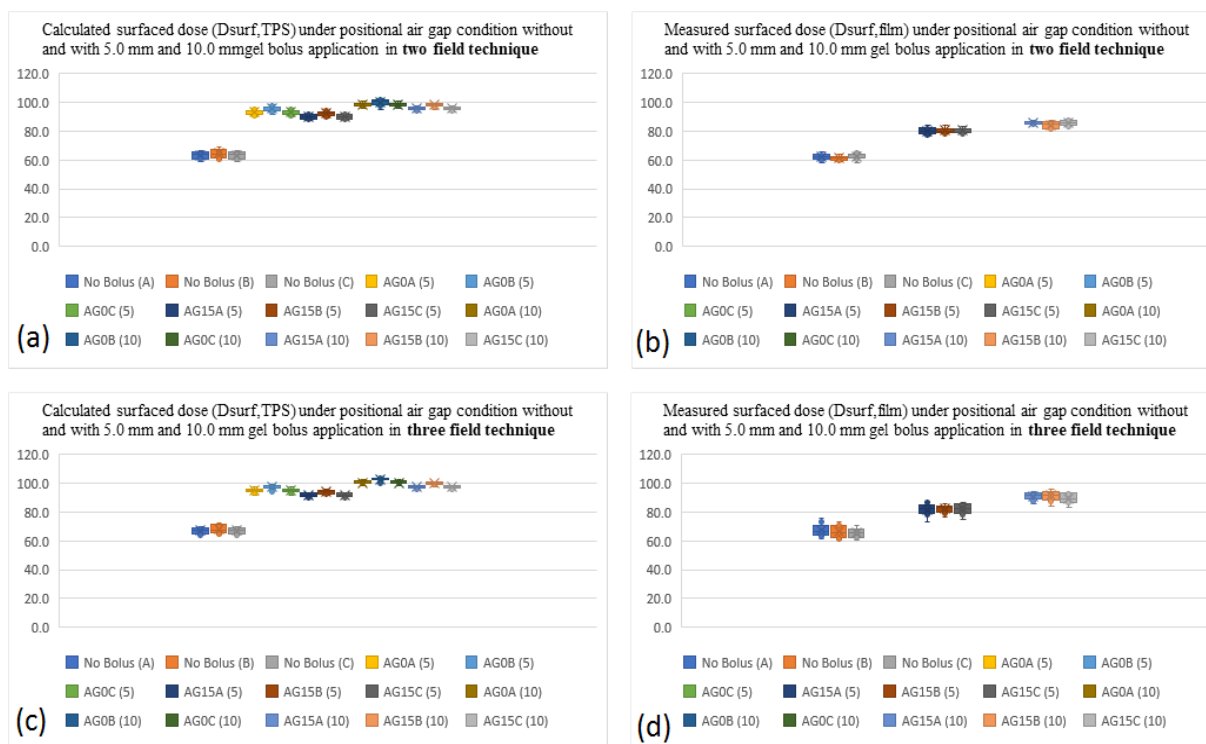


Figure 5. (a to d) Represents the Whisker Plots of $D_{surf,TPS}$ and $D_{surf, film}$ Surface Doses Measured in Presence of Non-uniform Air Gap Condition under No Bolus, 5.0 mm and 10.0 mm Bolus Application with Two and Three Field Technique at Slots A, B and C. As observed from the figure, there is reduction in surface dose as air gap thickness increases from 0.0 mm to 15.0 mm under both bolus and treatment techniques.

Table 4. Reduction of Surface Dose ($D_{surf,TPS}$ and $D_{surf, film}$) under 5.0 mm and 10.0 mm Bolus Thicknesses Without and with Uniform Air Gap Observed in Two Field and Three Field Treatment Techniques Towards Superior Portion of Thorax Phantom

Bolus thickness (in mm)	Treatment technique	Reduction in surface dose (%)					
		AG0 vs AG5		AG0 vs AG10		AG0 vs AG15	
		$D_{surf,TPS}$	$D_{surf, film}$	$D_{surf,TPS}$	$D_{surf, film}$	$D_{surf,TPS}$	$D_{surf, film}$
5	2 field	4.7	3.7	9.3	6.3	14	9.5
	3 field	4.9	5.8	9.8	11.3	14.7	16.2
10	2 field	6.1	5.9	10.5	8.6	15.2	12.4
	3 field	6.9	7.4	11.6	12.5	17.4	18.4

AG0, Air gap 0.0 mm; AG5, Air gap 5.0 mm; AG10, Air gap 10.0 mm; AG15, Air gap 15.0 mm

reported D_{surf} values in Table 3 for nil, 5.0 mm, and 10.0 mm bolus applications are in good agreement with the above-mentioned published literature. The calculated surface doses were found to be within 10% of the measured values in the absence of a bolus.

Specific to in bolus applications to irregular surface geometries, the skin dose measurements in air gaps under bolus gives us valuable information. Many studies have reported the effects of air gaps under a bolus on surface dose (Buston et al., 2000; Boman et al., 2000; Khan et al., 2013; Madhavi et al., 2015).

Butson et al. (Butson et al., 2000) reported that a 10.0 mm air gap under the bolus can reduce the surface dose by up to 10% for 6 MV static beams using parallel plate chamber with small-sized and/or 600 angled fields. Boman et al. (Boman et al., 2018) explored the dosimetric impact of surface dose with uniform air gap thicknesses of 5.0 mm & 10.0 mm below the 5.0 mm thick gel bolus

in Volumetric arc Therapy (VMAT) as well standard practice in field techniques in PMRT patients. They observed that the air gap of 10.0 mm under the bolus in VMAT plans reduced the surface dose up to 13.6% and which would result in the clinical impact on recurrence rate. Madhavi et al. (Madhavi et al., 2015) reported that an air gap of 5.0 mm thickness under the 5.0 mm thick gel bolus reduced the surface dose by 9% in head and neck treatments as observed from treatment planning system (TPS). Khan et al. (Khan et al, 2013) demonstrated that, for a 6 MV beam, reduction of surface dose (by about 10%) becomes significant for air gaps > 5.0 mm below gel bolus during IMRT therapy plans. By using a Markus parallel-plate chamber and a metal-oxide semiconductor field-effect transistor (MOSFET) dosimeter, Jin-Beom Chung et al. (Chung et al., 2013) investigated the effects on surface dose from air gaps of up to 10.0 mm under the 5.0 mm and 10.0 mm thick boluses in oblique 6

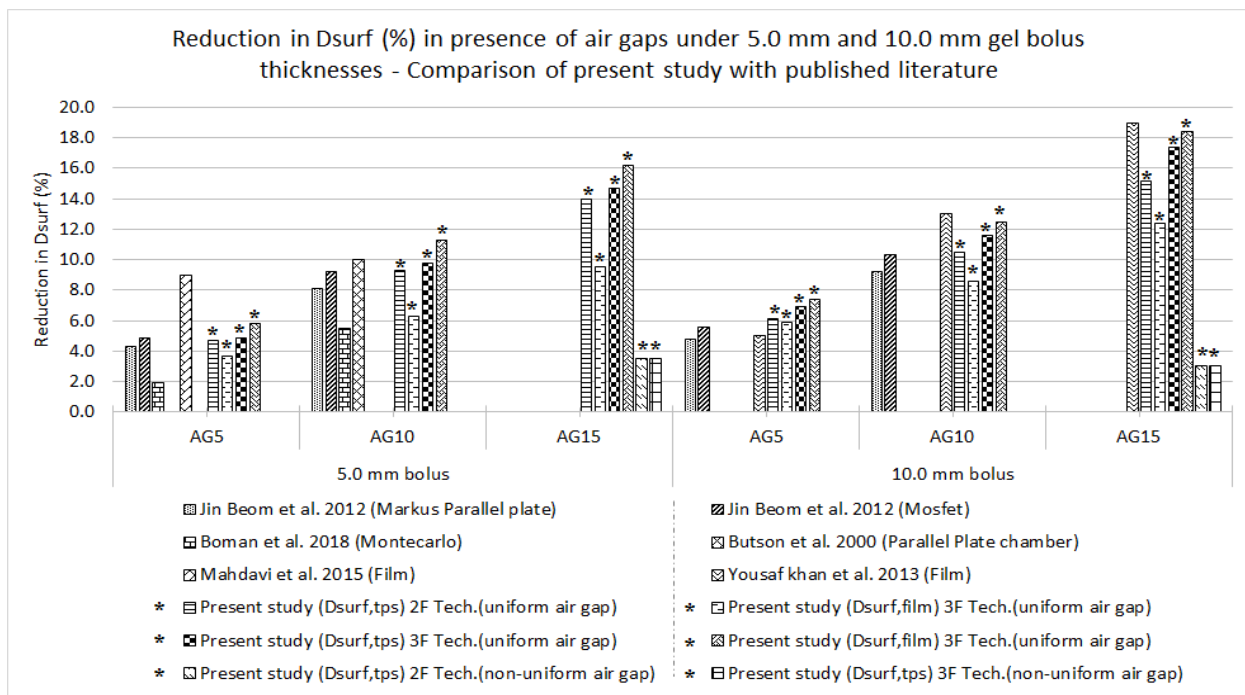


Figure 6. Reduction in D_{surf} (%) in Presence of Air Gaps under 5.0 mm and 10.0 mm Gel Bolus Thicknesses – Comparison of Present Study with Published Literature

Table 5. Overall Reduction in Surface Dose ($D_{surf, tps}$ and $D_{surf, film}$) under 5.0 mm and 10.0 mm Bolus Thicknesses without and with Air Gap Observed in Two Field and Three Field Treatment Techniques Towards Inferior Portion of Thorax Phantom at Three Slots A, B and C Inclusive.

Bolus thickness (in mm)	Treatment technique	Reduction in surface dose (%) [AG0 vs AG15]					
		A		B		C	
		$D_{surf, tps}$	$D_{surf, film}$	$D_{surf, tps}$	$D_{surf, film}$	$D_{surf, tps}$	$D_{surf, film}$
5	2 field	3.5	*	3.5	*	3.5	*
	3 field	3.5	*	3.5	*	3.5	*
10	2 field	3	*	3	*	3	*
	3 field	3	*	3	*	3	*

* Measurements were not made; AG0, Air gap 0.0 mm; AG15, Air gap 15.0 mm

MV photon beams with solid water phantom. With 600 angle incidence, they observed about 9.2% and 10.3% reduction of surface dose with 10.0 mm air gap under 5.0 mm and 10.0 mm bolus applications respectively. All the above studies addressed the D_{surf} reduction in various treatment techniques in presence of uniform air gaps under the gel bolus. Our outcome values of D_{surf} at different thickness of bolus applications with air gaps agree with the above published literature. However, in presence of non-uniform air gap condition, the surface dose reduction was minimal (3 to 3.5%) compared with the uniform air gap condition. So-Yeon Park et al. (Part et al., 2016) compared the 3D-printed bolus and commercial bolus in PMRT. They observed the average surface dose difference of -3.2% vs -1.1% with 5.0 mm commercial bolus vs 5.0 mm 3D printed (prepared with polylactic acid - PLA) bolus respectively, indicating that the 3D-printed bolus could not only reduce the daily positioning error, but also overcome the dose reduction caused by the air gap between the bolus and skin surface. Our study outcomes on reduction in D_{surf} in presence of air gaps under 5.0 mm and

10.0 mm gel bolus thicknesses with published literature were compared is as shown in Figure 6.

In our surface dose measurements, virtual bolus conditions could not be simulated due to non-availability of 3D printed bolus and the results reported are for 6 MV beam. Only 15.0 mm non-uniform air gap size across left side chest wall was created and the D_{surf} under different thicknesses of gel bolus was analyzed. However, by creating random sizes of air gaps and positions, like those occurring in PMRT treatments with bolus application, one can analyze the impact of surface dose in presence of air gap under bolus with different treatment techniques and photon energies.

In conclusion, based on our findings, when using gel bolus in PMRT treatments, special care must be taken to avoid unwanted air gaps under the bolus in order to avoid surface dose decrement and to achieve a uniform surface dose across the treatment region, where a customized 3D printed bolus may be a better option.

Author Contribution Statement

CS was the major contributor in literature search, designing and fabrication of the experiment, writing manuscript. DL, CS conducted the experiments. CS, RR, SB, AM, JS, AK and DL has corrected the manuscript subjectively, spelling and grammar check. CS is the main supervisor of the research and corresponding author. All authors read and approved the final manuscript.

Acknowledgements

Ethics approval

This study was conducted under the protocol approved by the Institutional Ethics Committee, Kasturba Medical College, Mangaluru (Reg.No.ECR/541/Inst/KA/2014).

Consent for publication

All of the authors declare that they have all participated in the design, execution, and analysis of the paper, and that they have approved the final version.

Availability of data and material not applicable.

Availability of data

Not applicable.

Conflicts of interest

The authors have no conflicts of interest to declare that are relevant to the content of this article.

References

- Bilge H, Cakir A, Okutan M, et al (2009). Surface dose measurements with GafChromic EBT film for 6 and 18MV photon beams. *Physica Medica*, **25**, 101–4.
- Boman E, Ojala J, Rossi M, et al (2018). Monte Carlo investigation on the effect of air gap under bolus in post-mastectomy radiotherapy. *Physica Medica*, **55**, 82–7.
- Butson MJ, Martin J, Cheung T, et al (2000). Effects on skin dose from unwanted air gaps under bolus in photon beam radiotherapy. *Radiat Measurements*, **32**, 201-204.
- Casanova Borca V, Pasquino M, Russo G, et al (2013). Dosimetric characterization and use of GAFCHROMIC EBT3 film for IMRT dose verification. *J Appl Clin Med Phys*, **14**, 4111.
- Chiu-Tsao S, Massillon-Jl G, Domingo-Muñoz I, et al (2012). SU-E-T-96: Energy Dependence of the New GafChromic-EBT3 Film's Dose Response-Curve. *Med Phys*, **39**, 3724.
- Chung Jin-Beom K, Jae-Sung K, In Ah L, et al (2013). Surface dose measurements from air gaps under a bolus by using a MOSFET dosimeter in clinical oblique photon beams. *J Korean Phys Soc*, **61**, 1143-7.
- Cox JD, Stetz J, Pajak TF (1995). Toxicity criteria of the Radiation Therapy Oncology Group (RTOG) and the European Organization for Research and Treatment of Cancer (EORTC). *Int J Radiat Oncol Biol Phys*, **31**, 1341-6.
- Fiedler DA, Hoffman S, Roeske JC, et al (2021). Dosimetric assessment of brass mesh bolus and transparent polymer-gel type bolus for commonly used breast treatment delivery techniques. *Med Dosim*, **46**, 10-4.
- Ha JS, Jung JH, Kim MJJ, et al (2016). Customized 3D Printed Bolus for Breast Reconstruction for Modified Radical Mastectomy (MRM). *Progress Med Phys*, **27**, 196.
- IAEA (2000). An international code of practice for dosimetry

based on absorbed dose to water, IAEA technical series No. 398, absorbed dose determination in external beam radiotherapy. Vienna: IAEA.

- Jreije A, Keshelava L, Ilickas M, et al (2021). Development of patient specific conformal 3D-printed devices for dose verification in radiotherapy. *Appl Sci*, **11**, 8657.
- Khan Y, Villarreal-Barajas JE, Udowicz M, et al (2013). Clinical and dosimetric implications of air gaps between bolus and skin surface during radiation therapy. *J Cancer Ther*, **4**, 1251–5.
- Lobo D, Banerjee S, Saxena P U, et al (2019). Clinical implementation of brass mesh bolus for chest wall postmastectomy radiotherapy and film dosimetry for surface dose estimates. *J Can Res Ther*, **15**, 1042–50.
- Lobo D, Challapalli S, Banerjee S, et al (2021). Fabrication and development of a thorax phantom to evaluate 3D CRT treatment planning techniques for post-mastectomy chest wall radiotherapy. *Phys Eng Sci Med*, **44**, 425-32.
- Mahdavi J, Petersen T, Sjölin M, et al (2015). PO-0838: Determination of the effect on patient surface dose from unwanted air cavities under bolus in VMAT. In 3rd ESTRO Forum, 2015.
- Ordóñez-Sanz C, Bowles S, Hirst A, et al (2014). A single plan solution to chest wall radiotherapy with bolus?. *Br J Radiol*, **87**, 20140035.
- Park SY, Choi CH, Park JM, et al (2016). A patient-specific polylactic acid bolus made by a 3D printer for breast cancer radiation therapy. *PLoS One*, **11**, e0168063.
- Robar JL, Moran K, Allan J, et al (2018). Inpatient study comparing 3D printed bolus versus standard vinyl gel sheet bolus for postmastectomy chest wall radiation therapy. *Pract Radiat Oncol*, **8**, 221-9.
- Sakai Y, Tanooka M, Okada W, et al (2021). Characteristics of a bolus created using thermoplastic sheets for postmastectomy radiation therapy. *Radiol Phys Technol*, **14**, 179-85.
- Wong G, Lam E, Bosnic, et al (2020). Quantitative effect of bolus on skin dose in postmastectomy radiation therapy. *J Med Imaging Radiat Sci*, **51**, 462-9.



This work is licensed under a Creative Commons Attribution-Non Commercial 4.0 International License.